

PACS numbers: 42.55.Wd; 42.81.Dp; 78.60.Lc
DOI: 10.1070/QE2015v045n02ABEH015414

Absorption and luminescence characteristics of $^5I_7 \leftrightarrow {}^5I_8$ transitions of the holmium ion in Ho^{3+}-doped aluminosilicate preforms and fibres

P.A. Ryabochkina, A.N. Chabushkin, A.F. Kosolapov, A.S. Kurkov

Abstract. **We have obtained the spectral dependences of the absorption cross sections for the Ho^{3+} $^5I_8 \rightarrow {}^5I_6$ and $^5I_8 \rightarrow {}^5I_7$ transitions in Ho^{3+}-doped aluminosilicate fibres and the spectral dependence of the stimulated emission cross section for the Ho^{3+} $^5I_7 \rightarrow {}^5I_8$ laser transition in Ho^{3+}-doped aluminosilicate fibre preforms. The lifetime of the Ho^{3+} $^5I_7$ upper laser level in the preforms has been determined.**

Keywords: *Ho^{3+} ions, aluminosilicate glass, optical fibres, luminescence, stimulated emission cross section.*

1. Introduction

In the last decade, considerable research effort has focused on holmium-doped fibre lasers and amplifiers. Interest in these devices is aroused by the fact that their emission spectrum lies at wavelengths above 2 μm, which offers the possibility of using them in medical applications. Moreover, the range 2.1–2.2 μm contains a local atmospheric window, suggesting that such lasers might be used in atmospheric optical communication, radar systems etc. To date, lasing in the range 2–2.21 μm has been demonstrated [1, 2], with the possibility of tuning the frequency [3]. The highest output power of a two-micron fibre laser has been 140 W [4], and the highest quantum efficiency has been 0.81 [5]. Chamorovskiy et al. [6, 7] reported a fibre laser operating on the Ho^{3+} $^5I_7 \rightarrow {}^5I_8$ transition and generating subpicosecond and femtosecond pulses. In addition, Antipov et al. [8] and Kamynin et al. [9] demonstrated efficient amplification of pulses of various powers.

Even though optically active silica fibres have been used to date to produce a variety of two-micron fibre lasers operating on the Ho^{3+} $^5I_7 \rightarrow {}^5I_8$ transition, the main spectroscopic characteristics of Ho^{3+} in silica glass (spectral dependence of the absorption cross section for the Ho^{3+} transition used for pumping two-micron emission, that of the stimulated emission cross section for the $^5I_7 \rightarrow {}^5I_8$ laser transition, and the lifetime of the Ho^{3+} $^5I_7$ upper laser level) have not yet been determined. Watekar et al. [10] made an attempt to determine them, but their results on the luminescence properties of Ho^{3+} ions in silica glass appear doubtful, because they found an absorption band around 1.75 μm and attributed it to the holmium ion, which has no appropriate optical transition in this spectral region. In view of this, it is of great current interest to determine the main spectroscopic characteristics of the holmium ion, especially for the $^5I_7 \rightarrow {}^5I_8$ laser transition of Ho^{3+} in silica glass, because this would allow one to construct adequate models for amplifiers and lasers with the aim of optimising their parameters.

In this paper, we report absorption and luminescence measurements for holmium ions in Ho^{3+}-doped aluminosilicate fibres and preforms. We obtained spectral dependences of the absorption cross sections for the $^5I_8 \rightarrow {}^5I_6$ and $^5I_8 \rightarrow {}^5I_7$ transitions and the stimulated emission cross section for the $^5I_7 \rightarrow {}^5I_8$ transition and determined the Ho^{3+} lifetime at the $^5I_7$ metastable level.

2. Materials and experimental procedure

In this study, we used silica preforms and optical fibres doped with holmium ions and alumina. They were fabricated by a standard chemical vapour deposition process (MCVD) and were solution-doped. The holmium concentration in the samples thus prepared ranged from 4.1×10^{19} to 1.2×10^{20} cm^{-3}. The Ho^{3+}concentration was determined by X-ray fluorescence analysis.

Figure 1 shows a partial energy level diagram of the Ho^{3+} ion. In optically active Ho^{3+}-doped fibres, the gain and lasing in the range 2.0–2.1 μm are due to the Ho^{3+} $^5I_7 \rightarrow {}^5I_8$ transition. Pumping is performed either to the $^5I_6$ level, and is then followed by nonradiative relaxation to the $^5I_7$ level, or directly to the $^5I_7$ level. To assess the spectral characteristics of these transitions, we measured the absorption spectra for the Ho^{3+} $^5I_8 \rightarrow {}^5I_6$ and $^5I_8 \rightarrow {}^5I_7$ transitions in Ho^{3+}-doped active fibre samples, assessed the holmium distribution across a preform, obtained the luminescence spectrum for the $^5I_7 \rightarrow {}^5I_8$ transition, and evaluated the decay kinetics of this luminescence in an aluminosilicate fibre preform.

The absorption spectra were obtained by the cut-back technique, using fibre pieces a few to tens of centimetres in length, differing in active ion concentration. The absorption spectrum was taken using an MDR-2 monochromator, a halogen lamp as a light source and an InGaAs photodetector, with an accuracy of 10% or better.

The Ho^{3+} distribution in the Ho^{3+}-doped active fibre preforms was assessed by X-ray fluorescence microanalysis.

P.A. Ryabochkina, A.N. Chabushkin N.P. Ogarev Mordovian State University, Bol'shevistkaya ul. 68, 430005 Saransk, Russia; e-mail: ryabochkina@freemail.mrsu.ru;
A.F. Kosolapov Fiber Optics Research Center, Russian Academy of Sciences, ul. Vavilova 38, 119333 Moscow, Russia;
A.S. Kurkov A.M. Prokhorov General Physics Institute, Russian Academy of Sciences, ul. Vavilova 38, 119991 Moscow, Russia; Photonics Laboratory, Perm Scientific Centre, Ural Branch, Russian Academy of Sciences, ul. Lenina 13a, 614990 Perm, Russia

Received 18 February 2014; revision received 12 May 2014
Kvantovaya Elektronika **45** (2) 102–104 (2015)
Translated by O.M. Tsarev

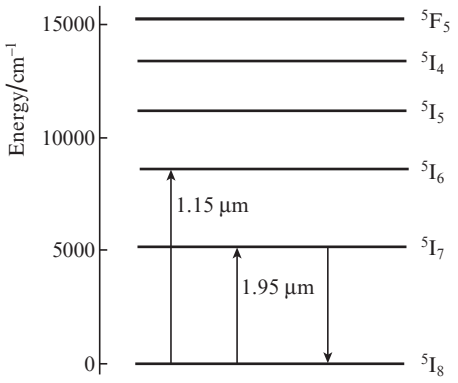

Figure 1. Partial energy level diagram of the Ho^{3+} ion in silica glass.

Ho^{3+} luminescence spectra of the aluminosilicate fibre preforms under cw laser excitation at $\lambda = 532$ nm were measured using an MDR-23 monochromator and a PbS-based photoresistor as a detector. The luminescence signal was synchronously detected by an SR-810 amplifier. The luminescence spectrum for the Ho^{3+} $^5I_7 \rightarrow {}^5I_8$ transition was corrected for the spectral response of the system.

Ho^{3+} $^5I_7$ luminescence decay kinetics in the aluminosilicate fibre preform were assessed during excitation of the Ho^{3+} $^5S_2$ level by a frequency-doubled Nd:YAG laser at a pulse duration of ~10 ns. The luminescence was detected by a PbS-based photoresistor with a time resolution of ~30 μs. Luminescence decay kinetics were followed using a GDS-720C digital oscilloscope.

3. Experimental results

Figure 2 shows the absorption spectrum of an aluminosilicate fibre doped with Ho^{3+} ions to a concentration of 4.1×10^{19} cm^{-3}. It is seen that the absorption peaks arising from the Ho^{3+} $^5I_8 \rightarrow {}^5I_6$ and $^5I_8 \rightarrow {}^5I_7$ transitions are located at wavelengths of 1.15 and 1.95 μm. Figure 3 shows a typical radial holmium distribution across a Ho^{3+}-doped active fibre preform. The measurements were made on five samples with a maximum active-ion concentration from 4.1×10^{19} to 1.2×10^{20} cm^{-3}.

In evaluating the absorption cross section, we took into account the convolution of the radial distributions of the

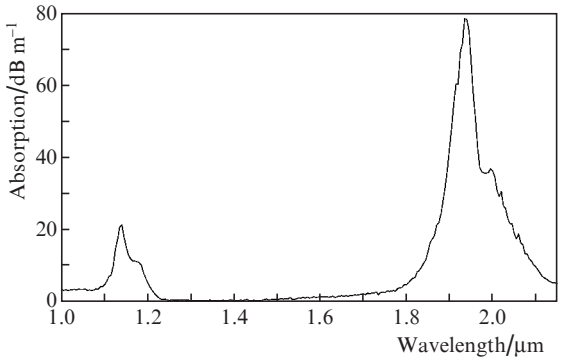

Figure 2. Absorption spectrum of an optical fibre doped with Ho^{3+} ions to a concentration of 4.1×10^{19} cm^{-3}.

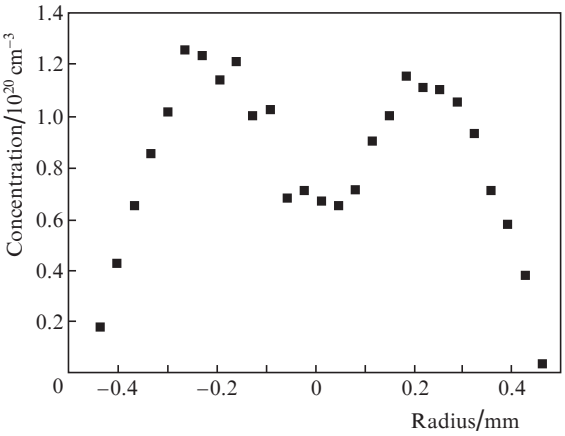

Figure 3. Radial Ho^{3+} distribution in an active fibre preform.

probe beam power and holmium concentration. From the spectral dependences of the absorption cross section, we obtained the following cross sections at the maxima of the absorption bands for the Ho^{3+} $^5I_8 \rightarrow {}^5I_6$ and $^5I_8 \rightarrow {}^5I_7$ transitions: $\sigma_{abs}(1.15\ \mu m) = 1.4 \times 10^{-21}$ cm^2 and $\sigma_{abs}(1.95\ \mu m) = 8.5 \times 10^{-21}$ cm^2. The absorption cross sections of the fibres differing in Ho^{3+} concentration differed by no more than 10%.

Figure 4 illustrates the luminescence decay kinetics for the Ho^{3+} $^5I_7 \rightarrow {}^5I_8$ transition during excitation to the $^5S_2$ level. The active-impurity concentration was 8×10^{19} cm^{-3}. The lifetime of the $^5I_7$ level, determined from a decrease in luminescence intensity I by a factor of e, was 7 ms.

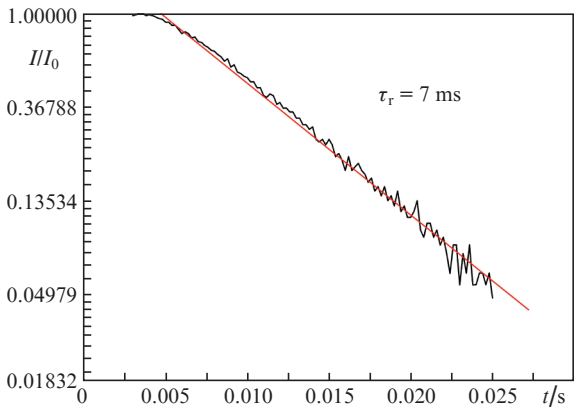

Figure 4. Luminescence decay kinetics for the Ho^{3+} $^5I_7 \rightarrow {}^5I_8$ transition in a Ho^{3+}-doped aluminosilicate fibre preform. The straight line represents a fit.

Given that the probability of the nonradiative relaxation of the $^5I_7$ level is rather low, we also determined its lifetime from the calculated probability A of the $^5I_7 \rightarrow {}^5I_8$ radiative transition:

$$\tau_r = 1/A. \tag{1}$$

The probability A was determined as

$$A = \frac{8\pi n_\lambda^2 c}{N\lambda^4} \frac{2J'+1}{2J+1} \int k(\lambda)\,d\lambda, \tag{2}$$

where $k(\lambda)$ is the absorption coefficient; J' and J are the total angular momenta of the 4f electrons in the ground and excited states (8 and 7, respectively); N is the Ho^{3+} concentration; $n_\lambda = 1.46$ is the refractive index of the medium; and λ is the wavelength of the transition.

Using Eqn (2), the lifetime of the Ho^{3+} $^5I_7$ level in the Ho^{3+}-doped aluminosilicate fibre was determined to be 6.7 ms, which agrees well with the lifetime $\tau_r = 7$ ms evaluated from the luminescence decay kinetic curve.

Figure 5 shows the spectral dependence of the stimulated emission cross section obtained for the Ho^{3+} $^5I_7 \rightarrow {}^5I_8$ laser transition in the Ho^{3+}-doped aluminosilicate fibre preforms using the Fuechtbauer–Ladenburg formula:

$$\sigma_e(\lambda) = \frac{\lambda^5}{8\pi c n_\lambda^2}\frac{1}{\tau_r}\frac{I(\lambda)}{\int \lambda I(\lambda d\lambda}. \quad (3)$$

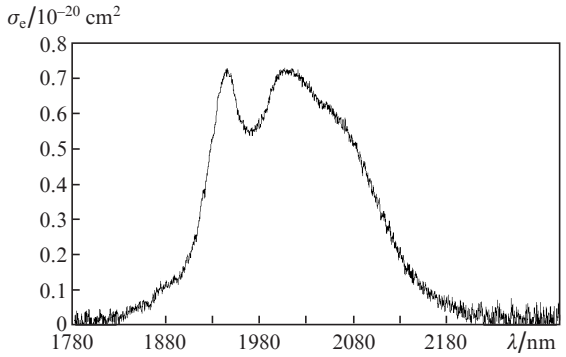

Figure 5. Spectral dependence of the stimulated emission cross section obtained for the Ho^{3+} $^5I_7 \rightarrow {}^5I_8$ laser transition in a Ho^{3+}-doped aluminosilicate fibre preform.

It is worth noting that formula (3) is often used to determine the stimulated emission cross section for a laser transition of the rare-earth ion in rare-earth-doped crystals. For example, it was used by Borik et al. [11] in studies of the luminescence properties of a ZrO_2–Y_2O_3–Ho_2O_3 crystal.

4. Conclusions

We have determined the main absorption and luminescence characteristics of the Ho^{3+} $^5I_7 \leftrightarrow {}^5I_8$ transitions in Ho^{3+}-doped aluminosilicate preforms and fibres and obtained spectral dependences of the absorption cross section for the Ho^{3+} $^5I_8 \rightarrow {}^5I_6$ and $^5I_8 \rightarrow {}^5I_7$ transitions in the aluminosilicate fibres. We have measured the lifetime of the $^5I_7$ upper laser level and found the spectral dependence of stimulated emission cross section for the Ho^{3+} $^5I_7 \rightarrow {}^5I_8$ laser transition. The present results can be used to optimise holmium-doped fibre lasers and amplifiers.

Acknowledgements. We are grateful to A.V. Marakulin, L.A. Minashina (Russian Federal Nuclear Center – Zababakhin All-Russia Research Institute of Technical Physics, Snezhinsk) and P.A. Rogozhnikov (Perm Scientific Industrial Instrument Making Company) for providing the preform and fibre samples.

This work was supported by the RF Ministry of Education and Science (state research target No. 0708 0210059 611: Organisation of Scientific Research).

References

1. Kurkov A.S., Sholokhov E.M., Medvedkov O.I., Dvoyrin V.V., Pyrkov Yu.N., Tsvetkov V.B., et al. *Laser Phys. Lett*., **6**, 661 (2009).
2. Antipov S.O., Kamynin V.A., Medvedkov O.I., Marakulin A.V., Minashina L.A., Kurkov A.S., Barannikov A.V. *Kvantovaya Elektron*., **43**, 603 (2013) [*Quantum Electron*., **43**, 603 (2013)].
3. Hemming A., Bennetts S., Simakov N., Davidson A., Haub J., Carter A. *Opt. Express*, **21**, 4560 (2013).
4. Kurkov A.S., Sholokhov E.M., Tsvetkov V.B., Marakulin A.V., Minashina L.A., Medvedkov A.S., Kosolapov A.F. *Kvantovaya Elektron*., **41**, 492 (2011) [*Quantum Electron*., **41**, 492 (2011)].
5. Kamynin V.A., Kablukov S.I., Raspopin K.S., Antipov S.O., Kurkov A.S., et al. *Laser Phys. Lett*., **9**, 893 (2012).
6. Chamorovskiy A.Yu., Marakulin A.V., Leinonen T., Kurkov A.S., Okhotnikov O.G. *Kvantovaya Elektron*., **42**, 12 (2012) [*Quantum Electron*., **42**, 12 (2012)].
7. Chamorovskiy A.Yu., Marakulin A.V., Ranta S., Tavast M., Rautiainen J., Leinonen T., Kurkov A.S., Okhotnikov O.G. *Opt. Lett*., **37**, 1448 (2012).
8. Antipov S.O., Kurkov A.S. *Laser Phys. Lett*., **10**, 125106 (2013).
9. Kamynin V.A., Antipov S.O., Barannikov A.V., Kurkov A.S. *Kvantovaya Elektron*., **44**, 161 (2014) [*Quantum Electron*., **44**, 161 (2014)].
10. Watekar P.R., Ju S., Han W.T. *J. Non-Cryst. Solids*, **354**, 1453 (2008).
11. Borik M.A., Lomonova E.E., Lyapin A.A., Kulebyakin A.V., Ryabochkina P.A., Ushakov S.N., Chabushkin A.N. *Kvantovaya Elektron*., **43**, 838 (2013) [*Quantum Electron*., **43**, 838 (2013)].